

FastBEV++: Fast by Algorithm, Deployable by Design

Yuanpeng Chen^{1*}, Hui Song^{1*}, Wei Tao¹, ShanHui Mo²

Shuang Zhang¹, Xiao Hua¹, TianKun Zhao¹

¹iMotion Automotive Technology (Suzhou) Co., Ltd ²Independent Researcher

Abstract

The advancement of camera-only Bird's-Eye-View (BEV) perception is currently impeded by a fundamental tension between state-of-the-art performance and on-vehicle deployment tractability. This bottleneck stems from a deep-rooted dependency on computationally prohibitive view transformations and bespoke, platform-specific kernels. This paper introduces FastBEV++, a framework engineered to reconcile this tension, demonstrating that high performance and deployment efficiency can be achieved in unison via two guiding principles: Fast by Algorithm and Deployable by Design. We realize the "Deployable by Design" principle through a novel view transformation paradigm that decomposes the monolithic projection into a standard Index-Gather-Reshape pipeline. Enabled by a deterministic pre-sorting strategy, this transformation is executed entirely with elementary, operator-native primitives (e.g., Gather, Matrix Multiplication), which eliminates the need for specialized CUDA kernels and ensures fully TensorRT-native portability. Concurrently, our framework is "Fast by Algorithm," leveraging this decomposed structure to seamlessly integrate an end-to-end, depth-aware fusion mechanism. This jointly learned depth modulation, further bolstered by temporal aggregation and robust data augmentation, significantly enhances the geometric fidelity of the BEV representation.

Empirical validation on the nuScenes benchmark corroborates the efficacy of our approach. FastBEV++ establishes a new state-of-the-art 0.359 NDS while maintaining exceptional real-time performance, exceeding 134 FPS on automotive-grade hardware (e.g. Tesla T4). By offering a solution that is free of custom plugins yet highly accurate, FastBEV++ presents a mature and scalable design philosophy for production autonomous systems. The code is released at: <https://github.com/ymlab/advanced-fastbev>.

1 Introduction

The evolution of autonomous driving is increasingly converging on camera-only Bird's-Eye-View (BEV) perception (Huang et al. 2021; Xie et al. 2022; and Wenhui Wang et al. 2022; Huang and Huang. 2022; Li et al. 2022; Liu et

al. 2022b). This paradigm, which transforms features from multi-camera image spaces into a unified BEV representation, offers a cost-effective and semantically rich foundation for critical downstream tasks such as 3D object detection and motion forecasting.

Despite its promise, a persistent dichotomy governs the BEV landscape, creating a trade-off between state-of-the-art accuracy and the tractability of on-vehicle deployment. This chasm is rooted in the architectural choices of the two dominant 2D-to-3D transformation paradigms. Query-based architectures (Phlion and Fidler 2020), predicated on the attention mechanism, implicitly demand specialized hardware acceleration for their core matrix operations, thereby limiting their portability across diverse compute platforms. In parallel, the influential Lift-Splat-Shoot (Phlion and Fidler 2020) paradigm introduced a depth-based transformation that relies on voxel pooling. While effective, this computational pattern is difficult to optimize on resource-constrained platforms, particularly those lacking a mature CUDA ecosystem. The high inference latency resulting from both design philosophies emerges as a fundamental impediment to real-world deployment.

The Fast-BEV (Huang et al. 2023) framework offered a seminal insight into resolving this tension. It empirically demonstrated that high-fidelity BEV representations could be attained without recourse to expensive depth or attention-based transformations. Its central contribution, the Fast-Ray transformation, established the viability of pre-computing the 2D-to-3D projection mapping as a static Look-Up Table (LUT). This design choice significantly reduced inference latency, providing a compelling proof-of-concept that performance and efficiency need not be mutually exclusive. However, the framework's architectural pattern implicitly coupled the pre-computed indices with a specific set of operational assumptions, motivating a more fundamental investigation into a truly hardware-agnostic transformation paradigm.

In this paper, we present FastBEV++, a framework that advances this line of inquiry. We posit that the aforementioned dichotomy can be fully reconciled by reframing the view transformation not as a monolithic, specialized operation, but as a sequence of standard, compiler-friendly tensor

*Equal Contribution.

Copyright © 2025, Association for the Advancement of Artificial Intelligence (www.aaai.org). All rights reserved.

manipulations. This thesis is embodied in two core principles: being Fast by Algorithm and Deployable by Design. Our work makes the following contributions:

- We introduce a novel view transformation methodology that decomposes the projection into a standard **Index-Gather-Reshape pipeline**. This design eliminates the dependency on bespoke kernels, enabling the **first fully TensorRT-Native implementation with zero custom plugins**.
- We demonstrate how this decomposed architecture uniquely facilitates a seamless, **depth-aware** fusion mechanism. By integrating learned depth priors directly into the gathering stage, we achieve significant performance gains without sacrificing deployment efficiency.
- We empirically validate that FastBEV++ establishes a new state-of-the-art on the nuScenes benchmark. Our results on production-grade hardware confirm that a principled focus on deployment tractability acts as a catalyst, rather than a constraint, for achieving superior perception accuracy.

2 Related Work

Camera-based BEV Perception The pursuit of robust 3D perception remains a cornerstone of autonomous driving research. While LiDAR-based methods (Shi, Wang, and Li 2019; Zhou and Tuzel 2018; Lang et al. 2019) have historically set performance benchmarks, their significant cost presents a substantial impediment to the democratization of autonomous technology. This has catalyzed a paradigm shift towards camera-only Bird’s-Eye-View (BEV) (Li et al. 2022; Wang et al. 2022) perception, a methodology that has demonstrated a remarkable capacity to yield semantically rich, spatially coherent 3D representations from inexpensive visual inputs. The canonical approach involves a view transformation that projects features from multiple, disparate camera perspectives into a unified, ego-centric BEV coordinate system. This unified representation serves as a foundational substrate for a gamut of downstream perceptual tasks, including 3D object detection and semantic map segmentation.

Architectural Trade-offs in View Transformation The pivotal component of the BEV paradigm is the 2D-to-3D view transformation, a module extensively explored in recent literature. While numerous seminal works have demonstrated impressive results on benchmarks like nuScenes, their architectural choices often exhibit inherent limitations concerning on-vehicle deployment tractability. These approaches largely diverge into two dominant philosophies.

Depth-Based Projection The influential Lift-Splat-Shoot (LSS) (Philon and Fidler 2020) paradigm established a methodology predicated on explicit per-pixel depth estimation. This approach “lifts” 2D features into 3D space by projecting them along camera rays according to a predicted depth distribution, followed by a “splatting” operation that aggregates these features into a rasterized BEV grid. While subsequent works like BEVDepth (Li et al. 2022)

and BEVFusion (Liu et al. 2022b) have refined this process with robust depth supervision, the paradigm’s reliance on a computationally intensive voxel pooling stage remains a critical bottleneck. This stage often necessitates bespoke, non-portable CUDA kernels for acceleration, rendering the approach intractable on resource-constrained platforms or those lacking a mature CUDA ecosystem.

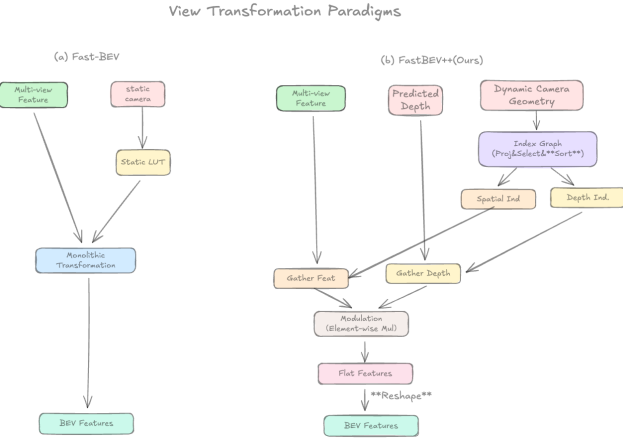
Query-Based Aggregation An alternative philosophy, epitomized by BEVFormer (adn Wenhui Wang et al. 2022), reframes view transformation as a process of information aggregation via learnable queries. A set of BEV queries interacts with multi-view image features through spatiotemporal attention mechanisms to construct the BEV representation. Although this obviates the need for explicit depth prediction, the quadratic complexity of the attention mechanism, as defined in Transformer, imposes a significant latency burden. This implicitly demands specialized hardware for efficient matrix multiplication, thereby constraining the model’s portability and real-time applicability—a challenge also noted in related works like PETR (Liu et al. 2022a) and DETR3D (Wang et al. 2022).

Rethinking Efficiency: The Pre-computation Paradigm of Fast-BEV The Fast-BEV framework (Huang et al. 2023; Li et al. 2024) offered a seminal insight into circumventing this performance-deployment trade-off. It was built upon the principles of earlier non-depth-based methods like M²BEV (Xie et al. 2022), and empirically demonstrated that high-fidelity BEV representations could be attained without recourse to either expensive Depth-Based Projection or Query-Based Aggregation. Its core contribution, the Fast-Ray transformation, established the viability of pre-computing the static geometric mapping from image coordinates to BEV voxels. By storing this projection as a Look-Up Table (LUT) and introducing a “Multi-View to One-Voxel” projection scheme, Fast-BEV dramatically reduced inference latency, providing a compelling proof-of-concept for deployment-oriented design.

However, the architectural pattern of Fast-BEV, while pioneering, is constrained by its reliance on a monolithic implementation that tightly couples geometry with static look-up tables. This limitation motivates a more foundational inquiry: Can the view transformation be reframed not merely as a pre-computed operation, but as a fully decomposed computational graph of elementary, hardware-agnostic primitives? This question constitutes the central thesis of FastBEV++. We transcend the original philosophy of static pre-computation by decomposing the entire transformation into a standard Index-Gather-Reshape pipeline. This principled decomposition unlocks a new tier of operator-native deployment efficiency. Moreover, it serves as a natural substrate for seamlessly integrating auxiliary cues, such as learned depth priors, allowing us to advance state-of-the-art performance without compromising deployment tractability.

3 Methodology

Our proposed framework, FastBEV++, is architected to reconcile the persistent dichotomy between state-of-the-art per-



formance and on-vehicle deployment tractability. This is achieved by reframing the view transformation not as a monolithic look-up operation, but as a fully decomposed computational graph composed of elementary, hardware-agnostic primitives. This principled design not only ensures unparalleled deployment-friendliness but also serves as a natural substrate for integrating auxiliary cues like predicted depth.

Figure 1: Conceptually contrasts our proposed FastBEV++ with the baseline Fast-BEV, highlighting a fundamental paradigm shift from monolithic to decomposed view transformation.

The baseline Fast-BEV (a) encapsulates the entire projection within a single, opaque operation dependent on static Look-Up Tables, creating a rigid coupling between geometry and feature extraction. In stark contrast, FastBEV++ (b) reframes this process as a transparent pipeline of standard operators. A dynamic geometry stage first computes a sparse Index Graph (via projection, selection, and sorting), which then orchestrates a feature aggregation stage composed entirely of hardware-native primitives (Gather, Element-wise Multiply). This decomposition is pivotal: it not only eliminates bespoke kernels—ensuring full TensorRT-Native compatibility—but also enables a seamless depth-aware modulation. The final reconstruction of dense BEV features is instantaneously achieved via a zero-cost Reshape (enabled by our pre-sorting strategy), underscoring the efficient, deployment-first philosophy of our design.

3.1 The Drawback of Monolithic View Transformation

The efficacy of the precomputation paradigm, pioneered by Fast-BEV, is well-established. However, its original formulation relies on a monolithic implementation where the entire 2D-to-3D transformation is abstracted as a single opaque operation Ψ :

$$\mathbf{V}(bev) = \Psi(\mathbf{F}(ing), LUT) \quad (1)$$

where $\mathbf{V}(bev)$ represents the BEV features, and LUT is the precomputed Look-UP-Table. This design creates a rigid

coupling between geometric mapping and feature gathering, leading to two critical deployment challenges:

1. Architectural Rigidity and Hardware Coupling: The black-box nature of Ψ fundamentally constrains the design space. It complicates the integration of auxiliary signals, such as predicted depth, in a principled, end-to-end manner. Furthermore, this abstraction implicitly couples the model with specific data structures, hindering portability across diverse hardware backends that may require distinct optimization strategies.

2. Implications for Memory Access Patterns: The feature gathering encapsulated within Ψ often results in non-contiguous memory access, which is notoriously inefficient on modern GPUs compared to coalesced access. More critically, traditional implementations typically rely on atomic operations (read-modify-write) for feature accumulation, causing severe serialization penalties. In contrast, our decomposed approach utilizes strictly read-only Gather operations, significantly improving memory throughput. As resolution scales, the monolithic approach becomes bandwidth-bound due to poor cache locality, creating a severe bottleneck for optimal hardware utilization.

3.2 FastBEV++: A Decomposed, Operator-Native Approach

The central contribution of our work, FastBEV++, is a principled engineering optimization designed to resolve these fundamental drawbacks. We posit that the key lies in the decomposition of the monolithic transformation Ψ . As we will now illustrate, this operation can be reframed as a two-stage computational graph composed entirely of elementary, hardware-agnostic primitives:

Stage 1: Generation of dynamic index graphs. The first stage computes a sparse mapping from BEV voxels to image pixels by inverting the standard projection pipeline. Crucially, we enforce a deterministic policy (e.g., sorting by voxel index) to resolve collisions, ensuring a strictly one-to-one mapping. This process yields two synchronized index tensors: $\mathcal{I}_{\text{spatial}}$ for image features and $\mathcal{I}_{\text{depth}}$ for depth probabilities.

$$\mathcal{M}(\mathbf{p}_v) \rightarrow \begin{cases} \mathcal{I}_{\text{spatial}} = \{(\text{cam}_k, u_k, v_k)\}_{k=1}^N \\ \mathcal{I}_{\text{depth}} = \{(\text{cam}_k, u_k, v_k, d_k)\}_{k=1}^N \end{cases} \quad (2)$$

Stage 2: Operator-Native Feature Aggregation With the index graph computed, the feature lifting is reformulated as a streamlined Index-Gather-Reshape pipeline.

Gather and Depth-Aware Modulation: Leveraging the decomposed nature of our pipeline, we perform feature extraction and depth fusion in a single, efficient step. We simultaneously gather the relevant semantic features and their corresponding depth probabilities using the synchronized indices, fusing them via element-wise modulation:

$$\mathbf{F}_{\text{flat}} = \underbrace{\text{Gather}(\mathbf{F}_{\text{img}}, \mathcal{I}_{\text{spatial}})}_{\text{Semantic Features}} \odot \underbrace{\text{Gather}(\mathbf{D}_{\text{prob}}, \mathcal{I}_{\text{depth}})}_{\text{Depth Weights}} \quad (3)$$

This process yields a flattened, depth-weighted feature tensor \mathbf{F}_{flat} , effectively injecting 3D geometric guidance into

Table 1: Comparison on the nuScenes val set. “L” denotes LiDAR, “C” denotes camera and “D” denotes Depth/LiDAR supervision. “||” indicates our method with scale NMS and test-time augmentation.

Methods	Image Res.	Modality	mAP \downarrow	mATE \downarrow	mASE \downarrow	mAOE \downarrow	NDS \uparrow
CenterPoint-Voxel (Jianwei Yin and Krahenbuhl, 2021)	-	L	0.564	-	-	-	0.648
CenterPoint-Pillar (Jianwei Yin and Krahenbuhl, 2021)	-	L	0.503	-	-	-	0.602
FCOS3D (Tai Wang and Lin, 2021)	900×1600	C	0.293	0.806	0.268	0.511	0.372
BEVDet-R50 (Junjie Huang and Du, 2021)	256×704	C	0.286	0.724	0.278	0.590	0.372
PETR-R50 (Yingfei Liu and Li, 2022)	384×1056	C	0.313	0.768	0.278	0.564	0.381
PETR-R50 (Yingfei Liu and Li, 2022)	512×1088	C	0.320	0.724	0.277	0.564	0.381
BEVDetD-Tiny (Huang and Huang, 2022)	256×704	C&D	0.323	0.674	0.272	0.503	0.453
BEVDepth-R50 (Yiniao Li and Li, 2022)	256×704	C&D	0.351	0.630	0.267	0.479	0.475
Fast-BEV-R50 (Bin Huang 2023)	256×704	C	0.347	0.660	0.285	0.472	0.473
Fast-BEV-R50 (Bin Huang 2023)	256×704	C	0.346	0.667	0.285	0.401	0.477
Fast-BEV++(R50)	256×704	C	0.344	0.656	0.285	0.512	0.478
Fast-BEV++(R50)	256×704	C&D	0.359	0.728	0.281	0.581	0.488
FCOS3D-R101 (Tai Wang and Lin, 2021)	900×1600	C	0.321	0.754	0.260	0.486	0.395
DETR3D-R101 (Y. Wang and Solomon 2022)	900×1600	C	0.347	0.765	0.267	0.392	0.422
EGO3D-R101 (Xiaoyi Li and Sun, 2022)	900×1600	C	0.402	0.727	0.272	0.542	0.454
MBEV-X101 (Enze Xie and Alvarez, 2022)	900×1600	C	0.417	0.647	0.275	0.377	0.470
PointFormer-T-R101 (Yanqin Jiang and Jiang, 2022)	900×1600	C	0.432	0.646	0.270	0.348	0.528
PETR-R101 (Yingfei Liu and Sun, 2022)	900×1600	C	0.401	0.660	0.276	0.368	0.496
DETR3D (Y. Wang and Solomon, 2022)	900×1600	C	0.303	0.860	0.278	0.437	0.374
BEVDet-Bas (Junjie Huang and Du, 2021)	512×1408	C	0.349	0.637	0.269	0.490	0.417
PETR-R101 (Yingfei Liu and Sun, 2022)	512×1408	C	0.346	0.710	0.270	0.420	0.421
BEVDepth-R50 (Huang and Huang, 2022)	640×1600	C	0.396	0.700	0.270	0.361	0.515
BEVFormer-R101 (Zhiqi Li and Dai, 2022)	900×1600	C	0.416	0.673	0.274	0.372	0.517
BEVDepth-R101 (Yiniao Li and Li, 2022)	512×1408	C&D	0.412	0.565	0.278	0.384	0.535
Fast-BEV-R50 (Bin Huang 2023)	900×1600	C	0.413	0.667	0.278	0.360	0.511
Fast-BEV-R101 (Bin Huang 2023)	900×1600	C	0.584	0.279	0.311	0.535	
Fast-BEV++(R101)	896×1600	C	0.397	0.633	0.284	0.513	0.507
Fast-BEV++(R101)	896×1600	C&D	0.414	0.603	0.276	0.501	0.522

the representation without incurring the cost of complex attention mechanisms.

Placement (Zero-cost Reshape): The final step “places” the gathered features into the dense BEV volume. Thanks to the pre-sorting in Stage 1, this is achieved instantaneously via a standard reshape operation, eliminating the need for expensive ReduceSum kernels:

$$\mathbf{V}_{\text{BEV}} = \text{Reshape}(\mathbf{F}_{\text{flat}}, [Z, H, W, C]) \quad (4)$$

This decomposition serves as the cornerstone of our framework’s hardware-agnostic portability.

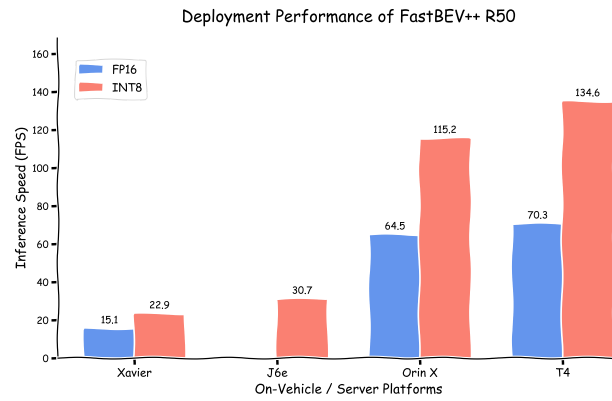
4 Experimental

We empirically validate our framework on the nuScenes val set against a spectrum of state-of-the-art methods. As shown in Table 1, our FastBEV++ demonstrates a superior balance between performance and efficiency. With a ResNet-50 backbone, our camera-only model achieves a competitive 0.478 NDS, surpassing both the original Fast-BEV (0.477 NDS) and the strong depth-based baseline, BEVDepth-R50 (0.475 NDS). This result corroborates that our decomposed, deployment-friendly view transformation enhances performance. When our end-to-end depth-aware fusion is activated (C&D modality), the performance is further elevated to 0.359 mAP and 0.488 NDS, significantly outperforming all counterparts with similar architectural complexity.

An ablation study was conducted to isolate the impact of our proposed modifications. As detailed in the table, when compared to the Fast-BEV-R101 baseline, our Fast-BEV++(R101) model demonstrates an improved mean Average Precision (mAP) of 0.414 over 0.413. This result highlights the effectiveness of the fastbev++ enhancements in refining the model’s feature representation for more accurate 3D object detection.

These findings suggest that a principled focus on deployment tractability, far from being a constraint, can act as a catalyst for developing more robust and ultimately superior perception systems.

Table1: Comparison on the nuScenes val set. “L” denotes LiDAR, “C” denotes camera and “D” denotes Depth/LiDAR supervision. “||” indicates our method with scale NMS and test-time augmentation Figure 2 illustrates the end-to-end inference speed, measured in frames per second (FPS), for



the quantization of FP16 and INT8. The results reveal two key findings. First, the framework demonstrates strong scalability, with performance increasing predictably in correspondence with the hardware’s computational capacity. Second, and more critically, the model exhibits substantial performance gains from INT8 quantization across all tested platforms. This is particularly evident on mainstream silicon such as the NVIDIA Orin X and T4, where inference speeds exceed 100 FPS. This pronounced susceptibility to low-precision optimization serves as strong evidence for the efficacy of our “Deployable by Design” philosophy. By architecting the view transformation with compiler-friendly primitives, FastBEV++ not only ensures portability but also effectively leverages the full acceleration potential of modern hardware, confirming its readiness for real-world, production-level deployment. Figure2 presents an empirical validation of our framework’s on-vehicle performance, benchmarking the end-to-end inference speed of the FastBEV++-R50 model. This evaluation spans a representative set of automotive-grade and server-class platforms and reports performance for both FP16 and INT8 quantized models.

Experimental Setup Our main model, FastBEV++-R50-CBGS, establishes a new state-of-the-art in the trade-off between accuracy and efficiency, achieving 0.489 NDS on the nuScenes validation set while running at 134 FPS on a Tesla T4 GPU with INT8 quantization. This performance is achieved by training the model for 20 epochs using the AdamW optimizer ($LR = 2e-4$, $WD = 1e-2$) with a warm-up and step decay schedule. The CBGS sampling strategy is also employed to handle the dataset’s long-tail distribution. All training was conducted on 8 GPUs with a total batch size of 64.

5 Conclusion

In conclusion, we presented FastBEV++, a framework that fundamentally challenges the trade-off between perception performance and deployment feasibility. Our core thesis—Fast by Algorithm, Deployable by Design—demonstrates that a principled focus on deployment constraints can catalyze, rather than limit, state-of-the-art performance.

We actualized this by reframing the view transformation into a standard Index-Gather-Reshape pipeline. This makes FastBEV++ the first fully TRT-Native (TensorRT-Native) framework requiring zero custom plugins, ensuring seamless deployment across diverse hardware platforms (e.g., NVIDIA Orin, Xavier, Tesla T4) without engineering overhead. Furthermore, this decomposed design uniquely enables an efficient, depth-aware fusion mechanism that proved critical for enhancing accuracy.

Our experiments on nuScenes establish a new benchmark for accuracy while maintaining exceptional real-time speeds on production-grade hardware. We hope this operator-native design philosophy sheds light on developing industrial-level perception that is both powerful and practical.

References

adn Wenhai Wang, Z. L.; Li, H.; Xie, E.; Sima, C.; Lu, T.; Yu, Q.; and Dai, J. 2022. Bevformer: Learning bird's-eye-view representation from multi-camera images via spatiotemporal transformers. In *arXiv preprint arXiv:2203.17270*.

Huang, J., and Huang., G. 2022. Bevdet4d: Exploit temporal cues in multi-camera 3d object detection. In *arXiv preprint arXiv:2203.17054*.

Huang, J.; Huang, G.; Zhu, Z.; and Du, D. 2021. Bevdet: High-performance multi-camera 3d object detection in bird-eye-view. In *arXiv preprint arXiv:2112.11790*.

Huang, B.; Li, Y.; Xie, E.; Liang, F.; Wang, L.; Shen, M.; Liu, F.; Wang, T.; Luo, P.; and Shao, J. 2023. Fast-bev: Towards real-time on-vehicle bird's-eye view perception. In *arXiv preprint arXiv:2301.07870*.

Lang, A. H.; Vora, S.; Caesar, H.; Zhou, L.; Yang, J.; and Beijbom, O. 2019. Pointpillars: Fast encoders for object detection from point clouds. In *in Proceedings of the IEEE/CVF conference on computer vision and pattern recognition, 2019*, pp. 12 697–12 705.

Li, Y.; Ge, Z.; Yu, G.; Yang, J.; Wang, Z.; Shi, Y.; Sun, J.; and Li, Z. 2022. Bevdepth: Acquisition of reliable depth for multi-view 3d object detection. In *arXiv preprint arXiv:2206.10092*.

Li, B.; Huang, Z.; Chen, Y.; Cui, F.; Liang, M.; Shen, F.; Liu, E.; Xie, L.; Sheng, W.; Ouyang, J.; and Shao. 2024. Fast-bev: A fast and strong bird's-eye view perception baseline. In *PAMI*.

Liu, Y.; Wang, T.; Zhang, X.; and Sun, J. 2022a. Petr: Position embedding transformation for multi-view 3d object detection. In *arXiv preprint arXiv:2203.05625*.

Liu, Z.; Tang, H.; Amini, A.; Yang, X.; Mao, H.; Rus, D.; and Han, S. 2022b. Bevfusion: Multi-task multi-sensor fusion with unified bird's-eye view representation. In *arXiv preprint arXiv:2205.13542*.

Philion, J., and Fidler, S. 2020. Lift, splat, shoot: Encoding images from arbitrary camera rigs by implicitly unprojecting to 3d. In *In European Conference on Computer Vision, pages 194–210*.

Shi, S.; Wang, X.; and Li, H. 2019. Pointrcnn: 3d object proposal generation and detection from point cloud. In *in Proceedings of the IEEE/CVF conference on computer vision and pattern recognition, 2019*, pp. 770–779.

Wang, Y.; V.C.Guizilini; Zhang, T.; Wang, Y.; Zhao, H.; and Solomon, J. 2022. Detr3d: 3d object detection from multi-view images via 3d-to-2d queries. In *in Conference on Robot Learning. PMLR, 2022*, pp. 180–191.

Xie, E.; Yu, Z.; Zhou, D.; Philion, J.; Anandkumar, A.; Fidler, S.; Luo, P.; and Alvarez, J. M. 2022. M2bev: Multi-camera joint 3d detection and segmentation with unified birds-eye view representation. In *arXiv preprint arXiv:2204.05088*.

Zhou, Y., and Tuzel, O. 2018. Voxelnet: End-to-end learning for point cloud based 3d object detection. In *in Proceedings of the IEEE conference on computer vision and pattern recognition, 2018*, pp. 4490–4499.